The Temperature Measurement of The Windings In a Three-Phase Electrical Motor Under Different Conditions

J. G. FANTIDIS[1,♣], D. V. BANDEKAS[1], K. KARAKOULIDIS[1],

G. LAZIDIS[1], C. POTOLIAS[1]

[1] *Department of Electrical Engineering, Institute for Technological Education, Kavala, Greece*

ABSTRACT

Based on a portable and high-resolution infrared thermographic system, this work studies the temperature measurement of the windings in a three phase electrical motor. The electrical machine operated under two scenarios, without load and under full-load conditions. The full-load scenario presents considerably higher temperatures and requires more time in order to reach a steady temperature state. In order to evaluate how an overload condition affects the temperature of the windings, we tested the machine under 10% overload for 15 minutes and the results proved that the temperature increases rapidly not only in the windings but also in the whole machine.

Keywords: Thermography; Electric motor; Overload; Fault diagnostics.

1. INTRODUCTION

Rotating electrical machines permeate all areas of industrial application which covers a broad range of machines. Owing to the requirement of increasing production in the manufacturing industry, rotating machinery is fundamentally required to run uninterruptedly for extended hours Without doubt today the unexpected failure of the electrical machines has become more costly and time-consuming than ever before. For these reasons, fault diagnosis of rotating machines is necessary [1-2]. In this direction a number of

methods has been developed and used, such as acoustic emission [3], eddy current [4], vibration analysis [5], wavelet transform (WT) [6], empirical mode decomposition (EMD) [7] frequency analysis [8] and infrared thermography [9].

Infrared thermography (IRT) is a non-destructive and visualizing technique which is becoming ever more popular in nondestructive testing of materials and structures. IRT provides useful and reliable information, particularly for preventive maintenance programs and on-line monitoring. With both rotating equipment and

♣Corresponding author, e-mail: fantidis@yahoo.gr

machinery IRT is often used to find immediate failures and critical problems [10]. About eighty percent (80%) of electrical motor failures are a result of winding damage in the motor stator, due to either overheating or voltage issues [11]. Fault detection in stator windings is an attractive topic nowadays [12]. The major goal of this work is to study the temperature of windings in a three phase induction motor under different operating conditions. All the measurements realized at the Institute of Technology of Kavala in the electrical machine laboratory.

2. FAILURE RATE MODEL FOR MOTOR WINDINGS

The operation principle of electrical machines is based on the interaction between the magnetic fields and the currents flowing in the windings of the machine. The life expectancy of a motor winding is mainly dependant on its operating temperature with respect to the permitted temperature rise of the winding. Temperature rise occurs in a motor owing to the losses that occur in the motor (copper and iron losses). The temperature inside the motor will depend on how effectively this heat can be removed by the cooling system of the motor. As amperage in the motor increases, the amount of heat on the windings increases. As a rule, it is estimated that a motor's life is reduced by 50% for every 10°C increase above the internal stator winding temperature limit [11]. The electric motor windings failure rate, λ_{WI}, is given by Equation (1)

$$\lambda_{WI} = \lambda_{WI,B} \cdot C_T \cdot C_V \cdot C_{alt} \qquad (1)$$

where: $\lambda_{WI,B}$ is the base failure rate of the electric motor windings, failures/million hours, C_T is the multiplying factor which considers the effects of ambient temperature on the base failure rate, C_V is the multiplying factor which considers the effects of electrical source voltage variations and C_{alt} is the multiplying factor which considers the effects of operation at extreme elevations [13].

3. PHYSICAL BASICS FOR IRT

The principle of IRT is based on the fact that every object with temperature above absolute zero (-273.15 °C) emits infrared radiated energy and exactly this energy is used to measure the temperature of the objects [1]. In physics, a blackbody is defined as an object which absorbs all radiation that falls on it at any wavelength. The spectral distribution of the radiation emitted by a black body is described by Planck's radiation law:

$$W_{\lambda b} = \frac{2\pi hc^3}{\lambda^5 (e^{hc/\lambda kT} - 1)} 10^{-6} [watt/m^2 \mu m] \qquad (2)$$

$W_{\lambda b}$ is blackbody spectral radiant emittance at wavelength λ, is the velocity of light, is Planck's constant, k is Boltzmann's constant, T is absolute temperature of the blackbody in Kelvin and λ is wavelength.

By integrating Planck's formula from $\lambda = 0$ to $\lambda = \infty$, total radiant emittance (Wb) of a blackbody can be obtained as (Stefan-Boltzmann formula)

$$W_b = \sigma \cdot T^4 \qquad (3)$$

which states that the total emissive power of a blackbody is proportional to the fourth power of its absolute temperature.

A more general case is of a non-blackbody, the one that doesn't absorb or emit the full amount of radiative flux. Instead, it radiates a portion of it, characterized by its emissivity, ε:

$$E = \varepsilon \cdot \sigma \cdot T^4 \qquad (4)$$

where E is the radiometric force and has dimensions of power density with unit joules per second per square meter (SI unit) or watts per square meter. ε is the remaining component of radiation after transmissivity (t) and reflectivity (ρ) are taken into account [14-15].

$$\varepsilon = 1 - (t+\rho) \qquad (5)$$

4. CASE STUDY

The thermographic system used for the measurement is a high-resolution, portable, digital-colour, infrared and visual camera with a noncooled Focal Plane Array microbolometer which is used as an infrared radiation sensor. The main specifications of the thermal camera are listed in Table 1. The thermographic system communicates with PC via FireWire (IEEE 1394) which are later processed in the suitable analysing software IRBIS® 3 professional. In the present work the temperature of the windings in a 3-phase slip-ring motor TERCO 1007 - 695 realized under different load conditions (Figure 1). The technical specifications of the motor are shown in Table 2 [16].

Table 1. Technical characteristics of the VarioCAM ® 7800 thermographic camera.

Parameter	Value
Spectral range	7.5 – 14 μm
Resolution	640 × 480 pixels (resolution enhancement onto 1280 × 960 pixels)
Temperature measuring range	-40 – 1200 °C
Temperature resolution at 30°C	Better than 0.08 K
Measurement accuracy	± 1.5 K (0 – 100 °C), ± 2% (< 0 and >100) °C
Emissivity	Adjustable from 0.1 to 1, in increments of 0.01
Spatial resolution/IFOV	0.8 mrad
Field of view/FOV	30° (H) ×23° (V)
Protection rating	IP54, IEC 529

Table 2. Motor Specifications

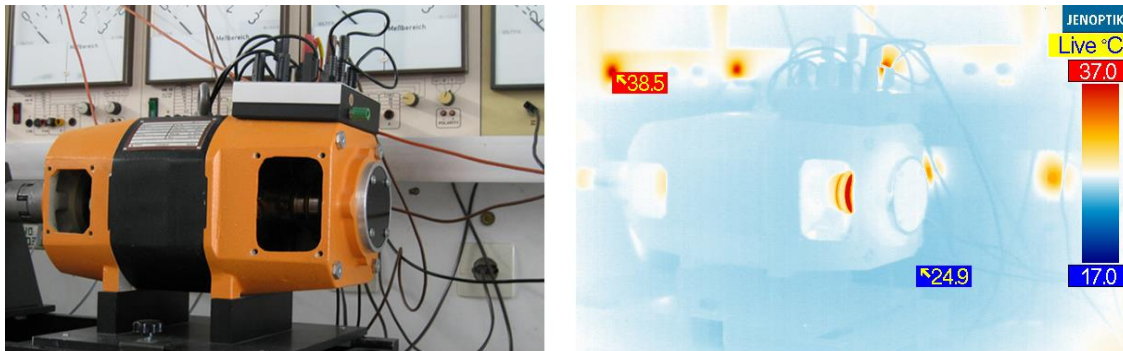| Parameter	Value
Power Supply	3 phase 690/400 V 1.7/3 A 50 Hz
Power	1.1 kW
Temperature Class	B (130°C)
Protection Class	IP23
Speed	1440 rpm
Weight	42 kg

Figure 1. The visual image (left) and the real thermal image (1 minute after the motor starts) of the tested motor

5. RESULTS AND DISCUSSION

With intention to study the average temperature in the windings of the machine the Terco 1007 - 695 motor was operated without load and for full load conditions for 200 minutes. Figure 2 illustrates the measured temperatures in the windings for both scenarios, with zero and with full load. As expected, in the case of full load the measured values are considerably higher. For zero load conditions the temperature in the windings will reach up to approximately 54 °C. It is clear from the measurements that without load the temperature increases rapidly during the first 30-40 minutes and with slower rate for the next minutes; it is practically steady after 2 hours of continuous operation. For full load the temperature in the windings after 200 minutes is above than 86 °C. Again the temperature rises rapidly in the first 30-40 minutes and with slower speed for the next minutes; however, it stops to increase only after approximately 3 hours of continuous operations. The real thermal images of the motor after 200 minutes of continuous operation are shown in Figure 3.
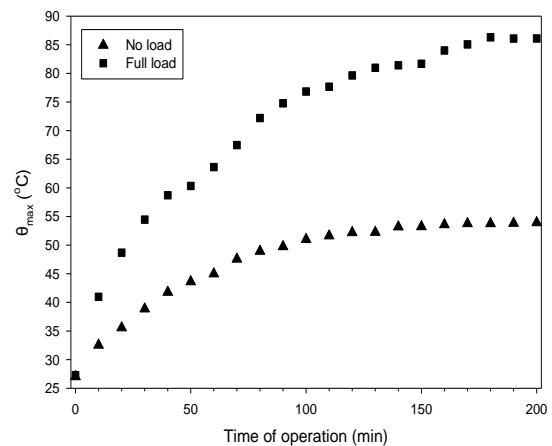

Figure 2. The measured temperatures in the windings for zero load and full load conditions.
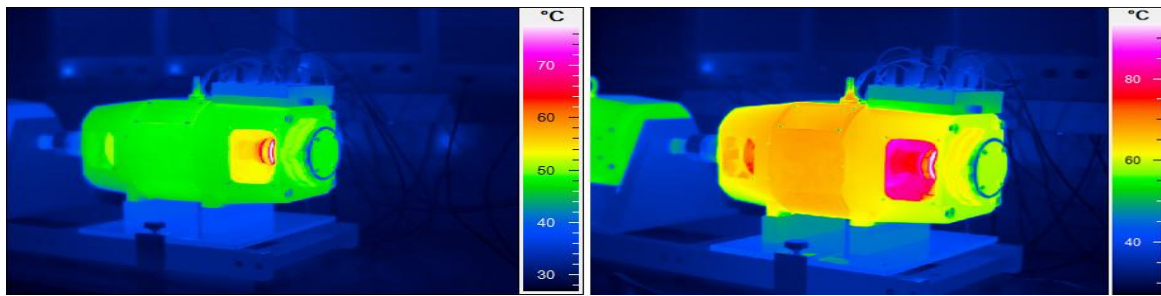
Figure 3. Thermal images of the motor after 200 minutes of operation for zero load (left) for full load (right).

With intention to evaluate how the maximum measured temperature changes during the time of operation the Terco 1007 - 695 induction motor was tested for 1.2 Ampere (without load) and for 3A (full load) conditions for 200 minutes. Figure 3.10 illustrates the fluctuation of the maximum measured values. It is apparent from Figure-10 that the temperature on the motor was raised steeply during the first 15 minutes. Generally about 40 minutes were required to reach a relevant steady state.
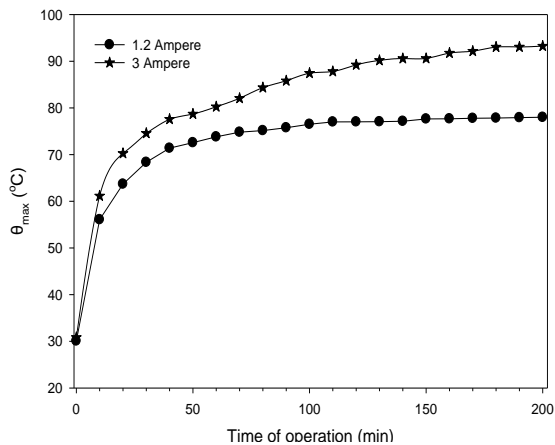

Figure 4. Fluctuations of the maximum measured values for 200 minutes of continue operation

In order to study explicitly the temperature rise at the first 40 minutes the two scenarios are realized with temperature measurements every minute. Figure 5 depicts average temperature in the windings for zero load. According to the Fig. 5, the temperature increase is almost linear. Figure 6 shows the corresponding results for full load conditions. According to this figure, there is a steep increment during the first 5 minutes and after that, the increase is again almost linear but with bigger slope.
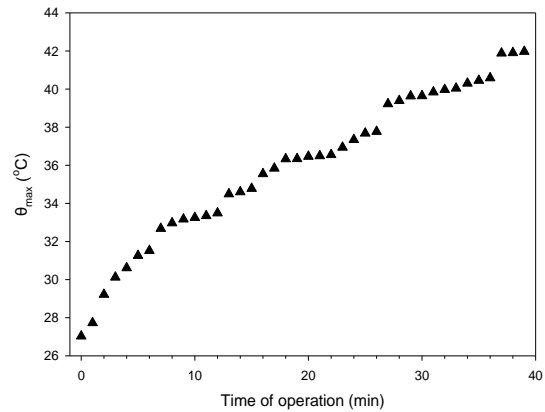

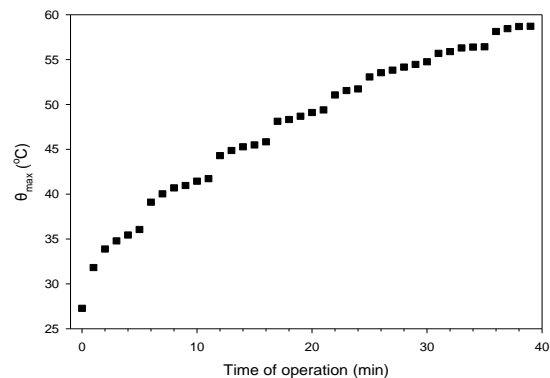Figure 5. The average measured temperature in the windings for zero load conditions.

Figure 6. The average measured temperature in the windings for full load conditions.

With the aim to consider the temperature in the windings under the overload conditions the next test was realized. After 90 minutes of continues operation with full load the electrical machine operates for 15 minutes with 10% overload. In comparison to that, the Figure 7 represents the temperature in the windings of the motor under full load and under 10% overloads. It is obvious that while for full load conditions the temperature increased less than 2.5 °C within 15 minutes, under the overload conditions the temperature increased sharply with gain more than 13 °C. Figure 8a shows the thermal image after 90 minutes of continuous operation with full load, the Figure 8b shows the real thermal image after 105 minutes of continuous operation with full load while the last

Figure 8c shows the thermal image after 90 minutes operation with full load plus 15 minutes operation with 10% overload. From the Fig. 8c the increase in the temperature in every point of the motor is evident.

With the aim to consider the temperature in the windings under the overload conditions the next test was realized. After 90 minutes of continues operation with full load the electrical machine operates for 15 minutes with 10% overload. In comparison to that, the Figure 7 represents the temperature in the windings of the motor under full load and under 10% overloads. It is obvious that while for full load conditions the temperature increased less than 2.5 °C within 15 minutes, under the overload conditions the temperature increased sharply with gain more than 13 °C. Figure 8a shows the thermal image after 90 minutes of continuous operation with full load, the Figure 8b shows the real thermal image after 105 minutes of continuous operation with full load while the last Figure 8c shows the thermal image after 90 minutes operation with full load plus 15 minutes operation with 10% overload. From the Fig. 8c the increase in the temperature in every point of the motor is evident.
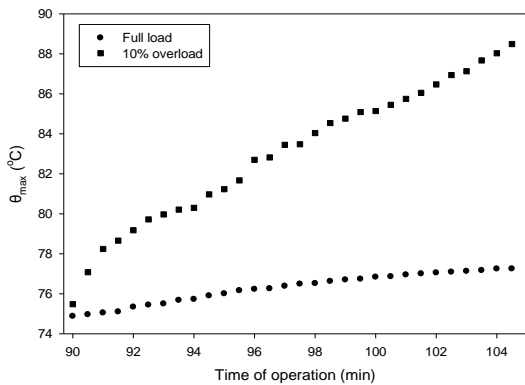

Figure 7. The temperature of the windings of the motor under full load and under 10% overload.
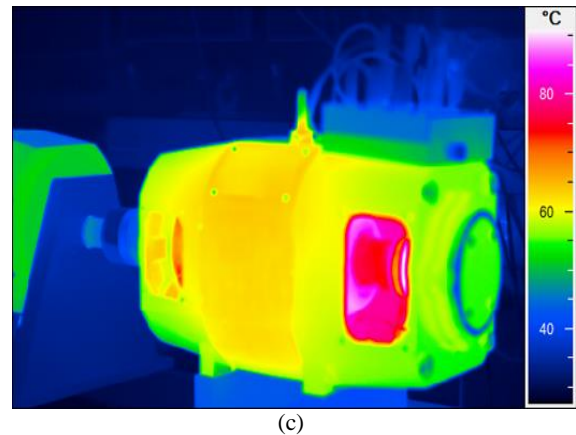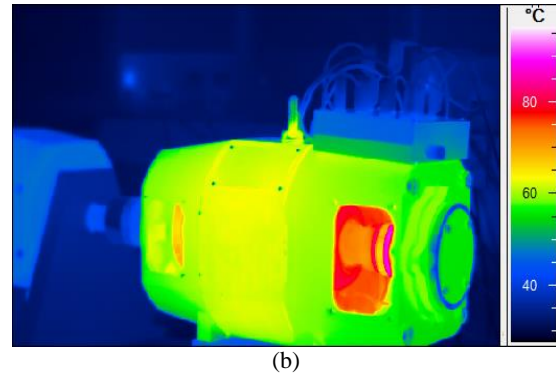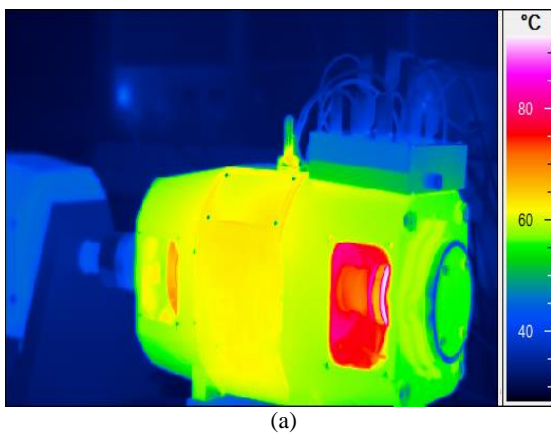

(a)

(b)

(c)

Figure 8. (a) The thermal image after 90 minutes operation with full load, (b) the thermal image after 105 minutes operation with full load (c) the thermal image after 90 minutes operation with full load plus 15 minutes operation with 10% overload.

6. CONCLUSIONS

Electrical machines play an important role in all sectors of the modern society such as the infrastructure, industries, service functions and the domestic sector. The failure of an electrical machine is common costly and for this reason the fault diagnosis capability against possible failures is necessary. IRT is a useful non-destructive method for the conditioned monitoring and diagnosis of rotating machinery. Because the most common reason for electrical motor failure is the winding damage this article focuses on the temperature measurement of the windings in a three phase motor under different scenarios using a portable and high-resolution infrared thermographic system.

REFERENCES

[1] Lei, Y., He, Z., Zi, Y., "A new approach to intelligent fault diagnosis of rotating machinery", Expert Systems with Applications 35: 1593–1600, (2008).

[2] Lei, Y., He, Z., Zi, Y., "Application of an intelligent classification method to mechanical fault diagnosis", Expert Systems with Applications 36: 9941–9948 (2009).

[3] Toutountzakis, T., Tan, C. K., Mba, D., "Application of acoustic emission to seeded gear

fault detection" NDT & E International, 38(1): 27–36 (2005).

[4] Liu, B., Ling, S. F., Gribonval, R., "Bearing failure detection using matching pursuit". NDT&E International, 35: 255–262 (2002).

[5] Yang B. S., Lim D. S., Tan, A. C. C., "VIBEX: an expert system for vibration fault diagnosis of rotating machinery using decision tree and decision table" Expert Systems with Application, 28(4): 735–742 (2005).

[6] Peng, Z. K., Chu, F. L., "Application of wavelet transform in machine condition monitoring and fault diagnostics: A review with bibliography". Mechanical Systems and Signal Processing, 17: 199–221, 2003.

[7] Huang, N. E., Shen, Z., Long, S. R., "The Empirical mode decomposition and the Hilbert spectrum for nonlinear and non-stationary time series analysis". Proceedings of the Royal Society of London, 454: 903–995. (1998).

[8] Lee, S. K., White, P. R., "Higher-order time-frequency analysis and its application to fault detection in rotating machinery". Mechanical Systems and Signal Processing, 11(4): 637–650 (1997).

[9] Younus, A. MD., Yang, B., "Intelligent fault diagnosis of rotating machinery using infrared thermal image", Expert Systems with Applications 39: 2082–2091 (2012).

[10] Kad, R. S., "IR thermography is a Condition Monitor Technique in industry", International Journal of Advanced Research in Electrical, Electronics and Instrumentation Engineering, 2(3): 988-993 (2013).

[11] Zhang P., Lu B., Habetler T.G., "Active Stator Winding Thermal Protection for Ac Motors", Proceedings of IEEE IAS Pulp and Paper Industry Conference, Alabama, USA, (2009)

[12] Nandi, S., Toliyat, H. A. and Li, X., "Condition monitoring and fault diagnosis of electric motors—a review", IEEE Trans. on energy conversion, 20(4): 719-129, (2005).

[13] Carderock Division Naval Surface Warfare Center, "Handbook of Reliability Prediction Procedures for Mechanical Equipment" (2010).

[14] Barreira, E., de Freitas, V.P., Delgado, J.M.P.Q. and Ramos, N.M.M., "Thermography Applications in the Study of Buildings Hygrothermal Behaviour, Infrared Thermography", Dr. Raghu V Prakash (Ed.), ISBN: 978-953-51-0242-7 (2012).

[15] Stipetic, S., Kovacic, M., Hanic, Z., Vrazic, M., "Measurement of Excitation Winding Temperature on Synchronous Generator in Rotation Using Infrared Thermography", IEEE Transactions on Industrial Electronics, 59 (5): 2288-2298 (2012).

[16] Fantidis J. G., Karakoulidis K., Lazidis G., Potolias C., Bandekas D. V., "The study of the thermal profile of a three-phase motor under different conditions", ARPN Journal of Engineering and Applied Sciences, 8 (11): 892 – 899 (2013).